
SoundCTM: Uniting Score-based and Consistency Models for Text-to-Sound Generation

Koichi Saito
Sony AI
NY, USA
koichi.saito@sony.com

Dongjun Kim
Stanford University
CA, USA

Takashi Shibuya
Sony AI
Tokyo, Japan

Chieh-Hsin Lai
Sony AI
Tokyo, Japan

Zhi Zhong
Sony Group Corporation
Tokyo, Japan

Yuhta Takida
Sony AI
Tokyo, Japan

Yuki Mitsufuji
Sony AI, Sony Group Corporation
NY, USA

Abstract

Sound content is an indispensable element for multimedia works such as video games, music, and films. Recent high-quality diffusion-based sound generation models can serve as valuable tools for the creators. However, despite producing high-quality sounds, these models often suffer from slow inference speeds. This drawback burdens creators, who typically refine their sounds through trial and error to align them with their artistic intentions. To address this issue, we introduce Sound Consistency Trajectory Models (SoundCTM). Our model enables flexible transitioning between high-quality 1-step sound generation and superior sound quality through multi-step generation. This allows creators to initially control sounds with 1-step samples before refining them through multi-step generation. While CTM fundamentally achieves flexible 1-step and multi-step generation, its impressive performance heavily depends on an additional pretrained feature extractor and an adversarial loss, which are expensive to train and not always available in other domains. Thus, we reframe CTM’s training framework and introduce a novel feature distance by utilizing the teacher’s network for a distillation loss. Additionally, while distilling classifier-free guided trajectories, we train conditional and unconditional student models simultaneously and interpolate between these models during inference. We also propose training-free controllable frameworks for SoundCTM, leveraging its flexible sampling capability. SoundCTM achieves both promising 1-step and multi-step real-time sound generation without using any extra off-the-shelf networks. Furthermore, we demonstrate SoundCTM’s capability of controllable sound generation in a training-free manner.

1 Introduction

Sound content, including Foley sounds [Great Big Story, 2017, WIRED, 2023] and sound effects, is essential for multimedia works such as video games, music, and films. Foley artists create sounds such as footsteps, breaking glass, and environmental sounds using physical items or by mixing and splicing digital sounds aligned with the visuals of multimedia works. To enhance immersive experiences, sound creators strive to produce flexible, diverse, and high-quality sound content tailored to each project.

Sound generation models have a potential to be valuable tools for sound creators. Recent diffusion-based Text-to-Sound (T2S) models [Liu et al., 2023a,b, Ghosal et al., 2023, Huang et al., 2023b] have shown promising results. Some models can condition on other modalities [Luo et al., 2023,

Tang et al., 2023] or use a human-in-the-loop approach [Majumder et al., 2024]. Despite producing high-quality sounds, these models suffer from slow inference speeds due to the iterative sampling in Diffusion Models (DMs) [Sohl-Dickstein et al., 2015, Song et al., 2021, Karras et al., 2022]. Sound creators must iterate to ensure the generated sounds align with their creative intentions, a process requiring them to listen to each sample individually. In contrast to images, where creators can quickly determine if the samples meet their expectations, assessing sounds is time-consuming. Thus, slow inference adds a significant burden and time to the creative process. Addressing slow inference makes sound generation models more appealing to sound creators.

An initial attempt to address slow inference for DM-based sound generation models is ConsistencyTTA [Bai et al., 2023], which uses Consistency Distillation (CD) [Song et al., 2023] on T2S Latent Diffusion Models (LDMs) [Rombach et al., 2022]. However, ConsistencyTTA focuses on 1-step generation, losing the flexibility of balancing sample quality with inference speed (see Table 6). This is another crucial issue for creators who need accurate, high-quality samples after finding suitable conditions for the models. This limitation stems from CD’s training regime that learns anytime-to-zero-time jumps.

In this paper, we present the *Sound Consistency Trajectory Model (SoundCTM)*, a novel T2S model that offers flexible switching between 1-step high-quality sound generation and higher-quality multi-step generation. This is achieved through a training framework that learns anytime-to-anytime jumps and employs deterministic sampling as proposed in Consistency Trajectory Models (CTMs) [Kim et al., 2024]. Built on CTM’s framework, we address the limitations of the current CTM training framework (see Section 3), which heavily depends on domain-specific components to achieve notable generation performance. Specifically, we propose a novel domain-agnostic feature distance that uses a teacher’s network as a feature extractor for distillation loss (see Section 4.1). Furthermore, we distill classifier-free guided text-conditional trajectories with Classifier-Free Guidance (CFG) [Ho and Salimans, 2022] as a new condition for student models. We train both text-conditional and unconditional student models simultaneously and introduce a new scaling term to interpolate text-conditional and unconditional neural jumps for SoundCTM’s sampling (see Section 4.2).

In addition, we explore SoundCTM’s capabilities for controllable sound generation without additional training. Following the recent success of DITTO [Novack et al., 2024], which achieves state-of-the-art (SOTA) training-free controllable music generation performance by optimizing an initial noise of DMs, we address its significant generation time using SoundCTM’s 1-step generation. Furthermore, we also propose a loss-based guidance [Yu et al., 2023, Levy et al., 2023] framework for SoundCTM by leveraging its anytime-to-anytime jump capability, which is another major method of DM-based training-free controllable generation (see Section 5).

In the experiments, SoundCTM achieves SOTA 1-step generation performance without any fine-tuning or auxiliary neural networks. Under multi-step sampling, SoundCTM surpasses other T2S models with real-time generation on a single NVIDIA RTX A6000 (see Figure 1 and Table 4). Additionally, we demonstrate SoundCTM’s capability of training-free controllable sound generation. Lastly, but noteworthy, our new frameworks are also applicable to other modalities since they do not rely on domain-specific components. We believe SoundCTM can open a new door to significantly enhancing the efficiency of sound creation workflows with its fast, flexible, controllable, and high-quality generation. It also paves the way for real-time dynamic sound generation in live performances, exhibitions, and video games.

Our contributions are summarized as:

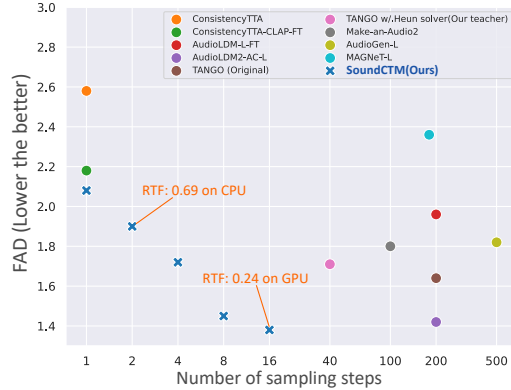


Figure 1: Performance comparison on AudioCaps testset. Real-time factors (RTFs) are measured on a single NVIDIA RTX A6000 and Intel Xeon CPU. SoundCTM can switch 1-step generation and multiple-step generation.

- We present SoundCTM, capable of flexibly switching between high-quality 1-step and higher-quality multi-step sound generation.
- To achieve high-quality sound generation, we address the limitations of the CTM’s training framework by proposing a novel domain-agnostic feature distance and methods for distilling classifier-free guided trajectories and using text-conditional and unconditional jump for sampling.
- We also explore SoundCTM’s capability for training-free controllable generation.

2 Preliminary

Diffusion Models Let p_{data} denote the data distribution. In DMs, the data variable $\mathbf{x}_0 \sim p_{\text{data}}$ is generated through a reverse-time stochastic process [Anderson, 1982] defined as $d\mathbf{x}_t = -2t\nabla \log p_t(\mathbf{x}_t)dt + \sqrt{2t}d\bar{\mathbf{w}}_t$ from time T to 0, where $\bar{\mathbf{w}}_t$ is the standard Wiener process in reverse-time. The marginal density $p_t(\mathbf{x})$ is obtained by encoding \mathbf{x}_0 along with a fixed forward diffusion process, $d\mathbf{x}_t = \sqrt{2t}d\mathbf{w}_t$, initialized by \mathbf{x}_0 , where \mathbf{w}_t is the standard Wiener process in forward-time. Song et al. [2021] present the deterministic counterpart of the reverse-time process, called the *Probability Flow* Ordinary Differential Equation (PF ODE), given by

$$\frac{d\mathbf{x}_t}{dt} = -t\nabla \log p_t(\mathbf{x}_t) = \frac{\mathbf{x}_t - \mathbb{E}_{p_{t|0}(\mathbf{x}|\mathbf{x}_t)}[\mathbf{x}|\mathbf{x}_t]}{t},$$

where $p_{t|0}(\mathbf{x}|\mathbf{x}_t)$ is the probability distribution of the solution of the reverse-time stochastic process from time t to 0, initiated from \mathbf{x}_t . $\mathbb{E}_{p_{t|0}(\mathbf{x}|\mathbf{x}_t)}[\mathbf{x}|\mathbf{x}_t] = \mathbf{x}_t + t\nabla \log p_t(\mathbf{x}_t)$ is a denoiser function¹ [Efron, 2011].

Practically, the denoiser $\mathbb{E}[\mathbf{x}|\mathbf{x}_t]$ is estimated by a neural network D_ϕ , obtained by minimizing a Denoising Score Matching (DSM) loss [Vincent, 2011, Song et al., 2021] $\mathbb{E}_{\mathbf{x}_0, t, p_{0|t}(\mathbf{x}|\mathbf{x}_0)}[\|\mathbf{x}_0 - D_\phi(\mathbf{x}, t)\|_2^2]$, where $p_{0|t}(\mathbf{x}|\mathbf{x}_0)$ is the transition probability from time 0 to t , initiated with \mathbf{x}_0 . Given the trained denoiser, the empirical PF ODE is given by

$$\frac{d\mathbf{x}_t}{dt} = \frac{\mathbf{x}_t - D_\phi(\mathbf{x}_t, t)}{t}. \quad (1)$$

DMs can generate samples by solving the empirical PF ODE, initiated with \mathbf{x}_T , which is sampled from a prior distribution π approximating p_T .

Text-Conditional Sound Generation with Latent Diffusion Models LDM-based T2S models [Liu et al., 2023a,b, Ghosal et al., 2023] generate audio matched to textual descriptions by first obtaining the latent counterpart of the data variable \mathbf{z}_0 through the reverse-time process conditioned by text embedding \mathbf{c}_{text} . This latent variable \mathbf{z}_0 is then converted to \mathbf{x}_0 using a pretrained decoder \mathcal{D} . During the training phase, D_ϕ is trained by minimizing the DSM loss $\mathbb{E}_{\mathbf{z}_0, t, p_{0|t}(\mathbf{z}|\mathbf{z}_0)}[\|\mathbf{z}_0 - D_\phi(\mathbf{z}, t, \mathbf{c}_{\text{text}})\|_2^2]$, where $p_{0|t}(\mathbf{z}|\mathbf{z}_0)$ is the latent counterpart of the transition probability from time 0 to t , initiated with \mathbf{z}_0 . \mathbf{z}_0 is given by a pretrained encoder as $\mathbf{z}_0 = \mathcal{E}(\mathbf{x}_0)$. We refer to Appendix A for a review of related work.

Consistency Trajectory Models CTMs predict both infinitesimally small step jump and long step jump of the PF ODE trajectory. $G(\mathbf{x}_t, t, s)$ is defined as the solution of the PF ODE from initial time t to final time $s \leq t$ and G is estimated by G_θ as the neural jump. To train G_θ , a *soft consistency matching* distillation loss (CTM loss) is introduced, comparing two s -predictions: one from a teacher ϕ and the other from a student θ as:

$$G_\theta(\mathbf{x}_t, t, s) \approx G_{\text{sg}(\theta)}(\text{Solver}(\mathbf{x}_t, t, u; \phi), u, s),$$

where $\text{Solver}(\mathbf{x}_t, t, s; \phi)$ is the pre-trained PF ODE in Eq. (1), a random $u \in [s, t]$ determines the amount of teacher information to distill, and sg is the exponential moving average (EMA) stop-gradient $\text{sg}(\theta) \leftarrow \text{stopgrad}(\mu \text{sg}(\theta) + (1 - \mu)\theta)$. To quantify the CTM loss between the student prediction $G_\theta(\mathbf{x}_t, t, s)$ and the teacher prediction $G_{\text{sg}(\theta)}(\text{Solver}(\mathbf{x}_t, t, u; \phi), u, s)$, the Learned Perceptual Image Patch Similarity (LPIPS) [Zhang et al., 2018] is used to measure a feature distance d_{feat} .

¹For simplicity, we omit $p_{t|0}(\mathbf{x}|\mathbf{x}_t)$, a subscript in the expectation of the denoiser, throughout the paper.

after transporting both predictions from s -time to 0-time as $\mathbf{x}_{\text{est}}(\mathbf{x}_t, t, s) := G_{\text{sg}(\theta)}(G_{\theta}(\mathbf{x}_t, t, s), s, 0)$ and $\mathbf{x}_{\text{target}}(\mathbf{x}_t, t, u, s) := G_{\text{sg}(\theta)}(G_{\text{sg}(\theta)}(\text{Solver}(\mathbf{x}_t, t, u; \phi), u, s), s, 0)$. Summarizing, the CTM loss is defined as

$$\mathcal{L}_{\text{CTM}}(\theta; \phi) := \mathbb{E}_{t \in [0, T]} \mathbb{E}_{s \in [0, t]} \mathbb{E}_{u \in [s, t]} \mathbb{E}_{\mathbf{x}_0} \mathbb{E}_{\mathbf{x}_t | \mathbf{x}_0} \left[d_{\text{feat.}}(\mathbf{x}_{\text{target}}(\mathbf{x}_t, t, u, s), \mathbf{x}_{\text{est}}(\mathbf{x}_t, t, s)) \right].$$

To enhance student learning, Kim et al. [2024] introduce two auxiliary losses, the DSM loss and an adversarial loss (GAN loss) [Goodfellow et al., 2014], defined as:

$$\mathcal{L}_{\text{DSM}}(\theta) = \mathbb{E}_{t, \mathbf{x}_0} \mathbb{E}_{\mathbf{x}_t | \mathbf{x}_0} [\|\mathbf{x}_0 - g_{\theta}(\mathbf{x}_t, t, t)\|_2^2],$$

and

$$\mathcal{L}_{\text{GAN}}(\theta, \eta) = \mathbb{E}_{\mathbf{x}_0} [\log d_{\eta}(\mathbf{x}_0)] + \mathbb{E}_{t \in [0, T]} \mathbb{E}_{s \in [0, t]} \mathbb{E}_{\mathbf{x}_0} \mathbb{E}_{\mathbf{x}_t | \mathbf{x}_0} [\log (1 - d_{\eta}(\mathbf{x}_{\text{est}}(\mathbf{x}_t, t, s)))],$$

where d_{η} is a discriminator. Therefore, the student model is trained with the following objective:

$$\mathcal{L}(\theta, \eta) := \mathcal{L}_{\text{CTM}}(\theta; \phi) + \lambda_{\text{DSM}} \mathcal{L}_{\text{DSM}}(\theta) + \lambda_{\text{GAN}} \mathcal{L}_{\text{GAN}}(\theta, \eta),$$

where λ_{DSM} and λ_{GAN} are scaling terms of the corresponding losses.

3 Limitations of CTM

Discriminator Selection Sensitivity for Performance Improvement Although CTMs demonstrate impressive 1-step image generation performance, this performance heavily depends on the GAN loss (See [Kim et al., 2024, Fig. 12]). However, obtaining performance improvements via the GAN loss requires careful selection of a discriminator. In fact, in our preliminary experiments, none of the off-the-shelf discriminators in the audio domain [gil Lee et al., 2023, Kumar et al., 2023, Shibuya et al., 2024, Iashin and Rahtu, 2021] lead better performance². Therefore, it is essential to develop a new methodology for high-quality sound generation that does not rely on the GAN loss.

Increase of Memory Consumption with CTM Loss for LDM Applying the CTM loss directly to LDM-based sound generation models results in substantial memory consumption. In the audio domain, the original CTM loss requires measuring a feature distance to obtain better performance using the Learned Perceptual Audio Patch Similarity (LPAPS)³ [Iashin and Rahtu, 2021] as a feature extractor, and \mathbf{z}_0 is required to be converted back to \mathbf{x}_0 through \mathcal{D} to align with the extractor’s input format. Additionally, despite the concept of LPAPS, there is no established checkpoint available⁴. Therefore, we propose a new framework that reduces memory consumption while maintaining the benefits of using the feature distance (see Section 4.1).

4 SoundCTM

To address the challenges of achieving fast, flexible, and high-quality T2S generation, we introduce SoundCTM by reframing the CTM’s training framework. Consistent with the CTM, we use the same distillation loss. Since this paper primarily illustrates the method using LDM-based T2S models as the teacher model, the student model is trained to estimate the neural jump G_{θ} as:

$$G_{\theta}(\mathbf{z}_t, \mathbf{c}_{\text{text}}, t, s) \approx G_{\text{sg}(\theta)}(\text{Solver}(\mathbf{z}_t, \mathbf{c}_{\text{text}}, t, u; \phi), \mathbf{c}_{\text{text}}, u, s),$$

where \mathbf{z}_t is the latent counterpart of \mathbf{x}_t , and $\text{Solver}(\mathbf{z}_t, \mathbf{c}_{\text{text}}, t, s; \phi)$ is the numerical solver of the pre-trained text-conditional PF ODE. To quantify the dissimilarity between G_{θ} and $G_{\text{sg}(\theta)}$, we propose a new feature distance in Section 4.1.

²This could be attributed to the lack of suitable for generative tasks in the audio domain.

³LPAPS is the audio variant of LPIPS. Other off-the-shelf pretrained networks such as VGGish [Hershey et al., 2017], PaSST [Koutini et al., 2022], and CLAP [Wu* et al., 2023] could be used as feature extractors. However, these models are trained at different sampling frequencies (16 kHz, 32kHz, and 48kHz, respectively), necessitating resampling the audio from the training data’s sampling frequency to that of the pretrained feature extractors. After resampling, the waveform must be transformed into another domain, such as the Mel-spectrogram domain, to match the input format of the extractors.

⁴The original checkpoint is no longer available according to the authors’ repository <https://github.com/v-iashin/SpecVQGAN/issues/13>.

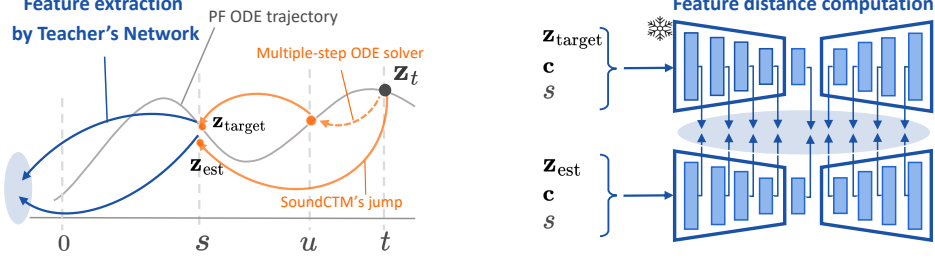


Figure 2: Illustrations of SoundCTM’s two predictions $\mathbf{z}_{\text{target}}$ and \mathbf{z}_{est} at time s with an initial value \mathbf{z}_t and the feature extraction by the teacher’s network for the CTM loss shown within the blue ellipse area. All the parameters of the teacher’s network are frozen. The conditional embedding \mathbf{c} and time s are also input to the feature extractor. Note that the teacher’s network does not need to follow the UNet architecture [Ronneberger et al., 2015]; a partial teacher’s network can also be used (see Table 3).

4.1 Teacher’s Network as Feature Extractor for CTM Loss

To address the limitations discussed in Section 3, we propose a new training framework that **utilizes the teacher’s network as a feature extractor** and measures the feature distance d_{teacher} for the CTM loss, as illustrated in Figure 2. Utilizing d_{teacher} offers two benefits:

Table 1: Difference of neural network function call between the distillation loss design

CTM loss design	s -time to 0-time projection	\mathbf{z}_0 to \mathbf{x}_0 projection
CTM [Kim et al., 2024]	Required	Required
SoundCTM	Free	Free

- We can reduce memory consumption by directly measuring the dissimilarity of the two predictions at s -time, avoiding the requirement to transport the teacher’s and student’s predictions from s -time to 0-time. This original CTM’s transportation is done by using $G_{\text{sg}(\theta)}(\cdot, \mathbf{c}_{\text{text}}, s, 0)$ and projecting \mathbf{z}_0 to \mathbf{x}_0 through \mathcal{D} , as shown in Table 1.
- Using d_{teacher} yields better performance compared with using the l_2 distance in the \mathbf{z} domain computed at either 0-time or s -time, as demonstrated in Section 6.

We define d_{teacher} between two predictions $\mathbf{z}_{\text{target}}$ and \mathbf{z}_{est} as follows:

$$d_{\text{teacher}}(\mathbf{z}_{\text{target}}, \mathbf{z}_{\text{est}}, \mathbf{c}, t) = \sum_{m=1}^M \|\text{TN}_{\phi, m}(\mathbf{z}_{\text{target}}, \mathbf{c}, t) - \text{TN}_{\phi, m}(\mathbf{z}_{\text{est}}, \mathbf{c}, t)\|_2^2, \quad (2)$$

where $\text{TN}_{\phi, m}(\cdot, \mathbf{c}, t)$ denotes the channel-wise normalized output feature of the m -th layer of the pretrained teacher’s network, conditioned by time t and embedding \mathbf{c} . This approach is feasible since noisy latents are input to the teacher’s network during teacher’s training.

4.2 CFG Handling for SoundCTM

To manage CFG in SoundCTM, we propose distilling the classifier-free guided PF ODE trajectory scaled by ω , uniformly sampled from the range $[\omega_{\min}, \omega_{\max}]$ during training, and using ω as a new condition in the student network, defined as:

$$G_{\theta}(\mathbf{z}_t, \mathbf{c}_{\text{text}}, \omega, t, s) = \frac{s}{t} \mathbf{z}_t + \left(1 - \frac{s}{t}\right) g_{\theta}(\mathbf{z}_t, \mathbf{c}_{\text{text}}, \omega, t, s).$$

The CTM loss for SoundCTM is formulated as:

$$\mathcal{L}_{\text{CTM}}^{\text{Sound}}(\theta; \phi) := \mathbb{E}_{t \in [0, T]} \mathbb{E}_{s \in [0, t]} \mathbb{E}_{u \in [s, t]} \mathbb{E}_{\mathbf{z}_0} \mathbb{E}_{\mathbf{z}_t | \mathbf{z}_0} \left[d_{\text{teacher}}(\mathbf{z}_{\text{target}}(\mathbf{z}_t, \mathbf{c}_{\text{text}}, \omega, t, u, s), \mathbf{z}_{\text{est}}(\mathbf{z}_t, \mathbf{c}_{\text{text}}, \omega, t, s), \mathbf{c}_{\text{text}}, s) \right], \quad (3)$$

where

$$\begin{aligned} \mathbf{z}_{\text{target}}(\mathbf{z}_t, \mathbf{c}_{\text{text}}, \omega, t, u, s) &:= G_{\text{sg}(\theta)}(\text{Solver}(\mathbf{z}_t, \mathbf{c}_{\text{text}}, \omega, t, u; \phi), \mathbf{c}_{\text{text}}, \omega, u, s), \\ \mathbf{z}_{\text{est}}(\mathbf{z}_t, \mathbf{c}_{\text{text}}, \omega, t, s) &:= G_{\theta}(\mathbf{z}_t, \mathbf{c}_{\text{text}}, \omega, t, s), \end{aligned}$$

$\text{Solver}(\mathbf{z}_t, \mathbf{c}_{\text{text}}, \omega, t, u; \phi) := \omega \text{Solver}(\mathbf{z}_t, \mathbf{c}_{\text{text}}, t, u; \phi) + (1 - \omega) \text{Solver}(\mathbf{z}_t, \emptyset, t, u; \phi)$, \emptyset is an unconditional embedding, and $\omega \sim U[\omega_{\min}, \omega_{\max}]$, respectively.

For auxiliary losses, as discussed in Section 3, we eliminate the GAN loss and use only the DSM loss, defined as:

$$\mathcal{L}_{\text{DSM}}^{\text{Sound}}(\theta) = \mathbb{E}_{t, \mathbf{z}_0, \omega} \mathbb{E}_{\mathbf{z}_t | \mathbf{z}_0} [\|\mathbf{z}_0 - g_{\theta}(\mathbf{z}_t, \mathbf{c}_{\text{text}}, \omega, t, t)\|_2^2] \quad (4)$$

Summing Eqs. (3) and (4), SoundCTM is trained with the following objective:

$$\mathcal{L}(\theta) := \mathcal{L}_{\text{CTM}}^{\text{Sound}}(\theta; \phi) + \lambda_{\text{DSM}} \mathcal{L}_{\text{DSM}}^{\text{Sound}}(\theta). \quad (5)$$

Following the original CTM, we employ adaptive weighting with $\lambda_{\text{DSM}} = \frac{\|\nabla_{\theta_L} \mathcal{L}_{\text{CTM}}^{\text{Sound}}(\theta; \phi)\|}{\|\nabla_{\theta_L} \mathcal{L}_{\text{DSM}}^{\text{Sound}}(\theta)\|}$, where θ_L is the last layer of the student’s network. Algorithm 2 summarizes SoundCTM’s training framework.

ν -interpolation for SoundCTM’s Sampling We introduce ν -interpolation in SoundCTM’s sampling, which linearly interpolates between the text-conditional and unconditional student models, given by:

$$\mathbf{z}_{s|t} = \nu G_{\theta}(\mathbf{z}_t, \mathbf{c}_{\text{text}}, \omega, t, s) + (1 - \nu) G_{\theta}(\mathbf{z}_t, \emptyset, \omega, t, s).$$

By adding ω as a new condition to the student network, the student model interpolates between the ω -conditioned text-conditional and ω -conditioned unconditional models during inference sampling. Algorithm 3 summarizes SoundCTM’s sampling framework, with the sampling timesteps denoted as $T = t_0 > \dots > t_N = 0$. We show the influence of ω and ν on the SoundCTM’s performance in Section 6.

5 Towards Training-free Controllable T2S Generation with SoundCTM

In the music domain, DITTO [Novack et al., 2024] that optimizing an initial noise latent \mathbf{z}_T of DMs achieves decent performance for training-free controllable music generation. Specifically, \mathbf{z}_T is optimized by

$$\mathbf{z}_T^* = \arg \min_{\mathbf{z}_T} \mathcal{L}(f(\mathbf{x}_0), \mathbf{y}_{\text{condition}}), \quad (6)$$

where \mathbf{z}_T^* is the optimized output, $f(\cdot)$ is a differentiable feature extractor that converts \mathbf{x}_0 into the same space as the target condition $\mathbf{y}_{\text{condition}}$, and $\mathbf{x}_0 = \mathcal{D}(\mathbf{z}_0)$. Although DITTO shows promising performance, it requires substantial time to generate a sample since \mathbf{x}_0 and \mathbf{z}_0 is given by the N -timestep reverse diffusion process in each optimization iteration⁵. Novack et al. [2024] also report the performance of a loss-based guidance method [Yu et al., 2023, Levy et al., 2023] as a baseline, which is another major method for controllable generation, using the same loss $\mathcal{L}(f(\mathbf{x}_0), \mathbf{y}_{\text{condition}})$, and DITTO outperforms the guidance-based method.

To explore SoundCTM’s capability for controllable generation in a training-free manner, we propose two new frameworks for SoundCTM based on \mathbf{z}_T -optimization and loss-based guidance. Firstly, we dramatically accelerate \mathbf{z}_T -optimization by utilizing SoundCTM’s 1-step generation, as shown in Algorithm 4, making each iteration N times faster than DITTO.

Loss-based Guidance Framework for SoundCTM In DMs, the loss-based guidance method involves an additional update $\mathbf{z}_{t-1} = \mathbf{z}_{t-1} - \rho_t \nabla_{\mathbf{z}_t} \mathcal{L}(f(\hat{\mathbf{z}}_0(\mathbf{z}_t)), \mathbf{y}_{\text{condition}})$ during sampling, where $\hat{\mathbf{z}}_0(\mathbf{z}_t)$ is a clean estimate derived from \mathbf{z}_t using Tweedie’s formula [Efron,

Algorithm 1 SoundCTM’s Loss-based Guidance Framework

Require: $\nu, \mathbf{c}_{\text{text}}, \mathbf{y}_{\text{condition}}, \omega, \gamma, \rho_{t_n}$

- 1: Start from \mathbf{z}_{t_0}
 - 2: **for** $n = 0$ to $N - 1$ **do**
 - 3: $\tilde{t}_{n+1} \leftarrow \sqrt{1 - \gamma^2 t_{n+1}}$
 - 4: Denoise $\mathbf{z}_{\tilde{t}_{n+1}} \leftarrow \nu G_{\theta}(\mathbf{z}_{t_n}, \mathbf{c}_{\text{text}}, \omega, t_n, \tilde{t}_{n+1})$
 - 5: $+ (1 - \nu) G_{\theta}(\mathbf{z}_{t_n}, \emptyset, \omega, t_n, \tilde{t}_{n+1})$
 - 6: $\mathbf{z}_{t_N|t_n} = G_{\theta}(\mathbf{z}_{t_n}, \mathbf{c}_{\text{text}}, \omega, t_n, t_N)$
 - 7: $\hat{\mathbf{y}}_{\text{condition}} = f(\mathcal{D}(\mathbf{z}_{t_N|t_n}))$
 - 8: $\mathbf{z}_{\tilde{t}_{n+1}} = \mathbf{z}_{\tilde{t}_{n+1}} - \rho_{t_n} \nabla_{\mathbf{z}_{t_n}} \mathcal{L}(\hat{\mathbf{y}}_{\text{condition}}, \mathbf{y}_{\text{condition}})$
 - 9: Diffuse $\mathbf{z}_{t_{n+1}} \leftarrow \mathbf{z}_{\tilde{t}_{n+1}} + \gamma t_{n+1} \epsilon$
 - 10: **end for**
 - 11: **Return** \mathbf{z}_{t_N}
-

⁵In their study, 20 diffusion steps are conducted per iteration, and the number of optimization steps ranges from 70 to 150, resulting in a total of approximately 1,400 to 3,000 diffusion steps.

2011], and ρ_t is a learning rate. We propose replacing $\hat{\mathbf{z}}_0(\mathbf{z}_t)$ with $\mathbf{z}_{0|t} = G_\theta(\mathbf{z}_t, \mathbf{c}_{\text{text}}, \omega, t, 0)$ and conducting loss-based sampling within SoundCTM’s γ -sampling, as shown in Algorithm 1. We denote the sampling timesteps as $T = t_0 > \dots > t_N = 0$.

By leveraging the anytime-to-anytime jump capability, SoundCTM can achieve both fast \mathbf{z}_T -optimization with 1-step sampling and multiple-step controllable generation with loss-based guidance within a single model. This is not possible with either a single Consistency Model (CM) [Song et al., 2023]-based T2S model or a DM-based T2S model.

6 Experiments

6.1 T2S Generation Performance

We evaluate SoundCTM on the AudioCaps dataset [Kim et al., 2019], which contains 47,289 pairs of 10-second audio samples and human-written text descriptions for the training set and 957 pairs for the testset. All audio samples are downsampled to 16 kHz. We adopt TANGO [Ghosal et al., 2023] as the teacher model trained with EDM’s variance exploding formulation [Karras et al., 2022]. We use $\gamma = 0$ for sampling and evaluate the model performance with student EMA rate $\mu = 0.999$.

Evaluation Metrics We use four objective metrics: the Frechet Audio Distance (FAD_{vgg}) [Kilgour et al., 2019] between the extracted embeddings by VGGish, the Kullback-Leibler divergence (KL_{passt}) between the outputs of PaSST [Koutini et al., 2022], a state-of-the-art audio classification model, the Inception Score (IS_{passt}) [Salimans et al., 2016] using the outputs of PaSST, and the CLAP score⁶. The lower FAD indicates better audio quality of the generated audio. The KL measures how semantically similar the generated audio is to the reference audio. The IS evaluates sample diversity. The CLAP score demonstrates how well the generated audio adheres to the given textual description.

Effectiveness of Utilizing Teacher’s Network as Feature Extractor

We first evaluate the efficacy of utilizing the teacher’s network as a feature extractor for the CTM loss by comparing the following cases: 1) the l_2 at 0-time step, 2) the l_2 at s -time step, and 3) the d_{teacher} at s -time step. We report the FAD of 1-step generation with $\omega = 3.5$ and $\nu = 1.0$ for inference. As shown in Table 2, the FAD of the d_{teacher} case is clearly better than the others. This result indicates that using d_{teacher} allows the student to distill the trajectory more accurately than using l_2 .

Additionally, we compare SoundCTM’s performance with the 1-step generation of ConsistencyTTA [Bai et al., 2023]. The FAD of SoundCTM’s 1-step generation trained with l_2 at 0-time step is 2.43, which is 0.15 points lower than that of ConsistencyTTA’s 1-step generation, as shown in Table 2. ConsistencyTTA is trained with the CD manner with the l_2 distance at the 0-time step of \mathbf{z} . This performance gap is likely due to differences in each teacher model. On the other hand, using d_{teacher} further boosts SoundCTM’s performance compared with using l_2 . This indicates that SoundCTM with d_{teacher} surpasses ConsistencyTTA even considering of the teacher difference.

Furthermore, we compare the results of using the teacher’s entire network with those of using the first half of it, as shown in Table 3. The results are not significantly different, indicating that there is potential that the model can reduce memory consumption by using only part of the teacher’s network without performance degradation.

Table 2: Performance comparisons among teacher and student models. DDIM sampling is used for TANGO-ConsistencyTTA and Heun solver is used for TANGO-EDM.

Model	# of steps	$\text{FAD}_{\text{vgg}} \downarrow$
Teacher Models		
TANGO-ConsistencyTTA (reported) (Teacher of ConsistencyTTA)	200	1.91
TANGO-EDM (Teacher of Ours)	40	1.71
Student Models		
ConsistencyTTA (reported)	1	2.58
SoundCTM w/ l_2 (0-time step)	1	2.43
SoundCTM w/ l_2 (s -time step)	1	2.45
SoundCTM w/ d_{teacher}	1	2.17

Table 3: Performance comparison on different architectures for feature extractors

Network architecture	# of steps	$\text{FAD}_{\text{vgg}} \downarrow$	$\text{IS}_{\text{passt}} \uparrow$	CLAP \uparrow
First half of UNet	1	2.18	7.15	0.43
	4	1.79	7.11	0.44
Entire UNet	1	2.18	7.18	0.43
	4	1.76	7.14	0.45

⁶We use the "630k-audioset-best.pt" checkpoint from <https://github.com/LAION-AI/CLAP>

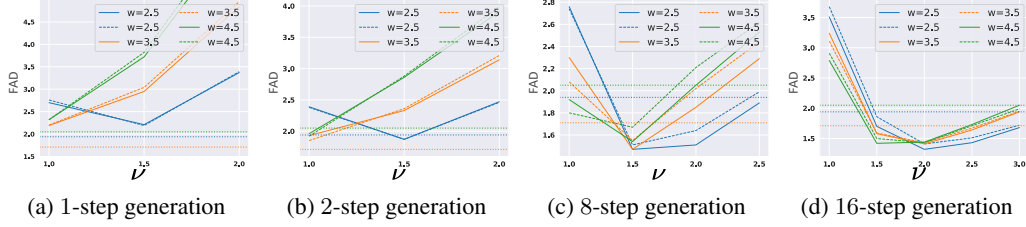


Figure 3: FAD for various ω and ν . The solid, dashed, dotted lines indicate the FAD of the students trained with $\omega \sim U[2.0, 5.0]$, the students trained with $\omega \sim U[1.5, 7.0]$, and the teachers.

Influence of ω and ν for SoundCTM’s Sampling We examine the influence of both ω and ν on SoundCTM’s performance. In Figure 3, we compare SoundCTM trained with $\omega \sim U[2.0, 5.0]$ to $\omega \sim U[1.5, 7.0]$ across various ω and ν values during inference. Overall, there is no significant difference in FAD between $\omega \sim U[2.0, 5.0]$ (solid line) and $\omega \sim U[1.5, 7.0]$ (dashed line). This suggests that precisely pre-defining the range of ω for the student training is not necessary. A wider range of ω can be used for student training when prior knowledge of the teacher’s dynamics of ω is absent, and high-quality generation can be achieved by adjusting ω and ν during inference.

The students show the better FAD than the best FAD of teachers through ν -interpolation during SoundCTM’s sampling. This result could be interpreted as ν allows for generating samples that are more favorable to the FAD in the conditional domain, as the pairs between c_{text} and the samples x_0 given the condition are many-to-many.

Performance Comparison with Other T2S Models We compare SoundCTM’s performance with other T2S models under both 1-step and multi-step generation. Here, we report the results of SoundCTM trained with more iterations (30 K iterations) compared with the previously mentioned results (18 K iterations). We employ AudioLDM-L-FT [Liu et al., 2023a], AudioLDM2-L [Liu et al., 2023b], TANGO [Ghosal et al., 2023], and ConsistencyTTA as our baseline models. Table 6 presents the quantitative results. All the DM-based models use DDIM sampling [Song et al., 2020] except for our teacher model. Under the 1-step generation setting, SoundCTM shows the best performance in all evaluation metrics. This achievement is the obtained from using d_{teacher} as discussed earlier. Note that ConsistencyTTA-CLAP-FT conducts extra fine-tuning to maximize the CLAP score using CLAP network after its CD training.

Under the multi-step case, there are clear trade-offs between the performance improvements and the number of sampling steps. We highlight these results are attributed to SoundCTM’s deterministic sampling ($\gamma = 0$) and anytime-to-anytime jump training framework, which cannot be achieved with the CD framework and its lack of deterministic sampling capability (See ConsistencyTTAs’ 2-step results in Table 6). In addition, SoundCTM demonstrates the state-of-the-art FAD and IS against all diffusion-based baselines with only 16 steps. The reason SoundCTM outperforms the teacher model at 8 and 16 steps is due to our ν -interpolation as discussed earlier. Note that all diffusion-based baselines use both text-conditional and unconditional predictions, the same setting as our 8 and 16-step generation.

Table 4: Inference speed and RTF. RTF < 1.0 indicates real-time generation.

Method	# of steps	Batch size	Speed [sec.]	RTF ↓
AudioLDM2-Large	200	1	80	8.0
	200	8	16.5	1.7
TANGO	200	1	24	2.4
SoundCTM on GPU	16	1	2.43	0.24
SoundCTM on CPU	2	1	6.93	0.69

Table 5: Quantitative results of sound intensity control on SoundCTM

# of steps	z_T optimization	Loss guidance	MSE↓	FAD _{vgg} ↓	CLAP ↑
Default 16-step T2S Generation	✗	✗	231.9	2.08	0.47
1	✓	✗	6.57	4.94	0.34
16	✓	✗	60.2	3.65	<u>0.38</u>
16	✗	✓	<u>18.5</u>	3.04	0.41

Generation Time Since one of our goals is to achieve real-time high-quality generation, we verified that our model can generate samples in real-time by measuring the inference time and real-time factors (RTFs) on a single NVIDIA RTX A6000. For reference, we also measure those of the original

Table 6: Performance comparisons on AudioCaps test set. Bold and underlined scores indicate the best and second-best results. \dagger denotes the results tested by us using the provided checkpoints by the authors, as not all metrics are provided in each paper. ω and ν denote the CFG scale and parameter for the ν -interpolation. $\nu = 1$ denotes only the text-conditional jump is used.

Model	# of sampling steps	ω	ν	FAD _{vgg} ↓	KL _{passt} ↓	IS _{passt} ↑	CLAP ↑
Diffusion Models							
AudioLDM-Large-FT [Liu et al., 2023a]	200	3.0	-	1.96	1.59	-	-
AudioLDM 2-AC-Large [Liu et al., 2023b]	200	3.5	-	<u>1.42</u>	0.98	-	-
AudioLDM 2-Full-Large [Liu et al., 2023b]	200	3.5	-	1.86	1.64	-	-
TANGO [†] [Ghosal et al., 2023]	200	3.0	-	1.64	1.31	6.35	0.44
TANGO w/. Heun Solver (Our teacher model)	40	3.5	-	1.71	1.28	<u>8.11</u>	0.46
Distillation Models							
ConsistencyTTA [Bai et al., 2023](reported)	1	5.0	-	2.58	-	-	-
ConsistencyTTA [†] (tested by us)	1	5.0	-	2.67	1.33	6.85	0.41
	2	5.0	-	3.18	1.34	7.12	0.38
ConsistencyTTA-CLAP-FT (reported)	1	3.0	-	2.18	-	-	-
ConsistencyTTA-CLAP-FT [†] (tested by us)	1	3.0	-	2.22	1.35	6.95	0.41
	2	3.0	-	2.38	1.32	7.15	0.40
SoundCTM(Ours)	1	3.5	1.0	2.08	1.26	7.13	0.43
	2	3.5	1.0	1.90	1.24	7.26	<u>0.45</u>
	4	3.5	1.0	1.72	1.22	7.37	<u>0.45</u>
	8	3.0	1.5	1.45	1.20	7.98	0.46
	16	3.0	2.0	1.38	<u>1.19</u>	8.24	0.46

TANGO and AudioLDM2-Large with a batch size of one⁷. The all three models are the top three in terms of the FAD in Table 6, based on the UNet architecture with similar parameter sizes, and generate the same duration of the samples (10-second audio). As shown in Table 4, SoundCTM can achieve real-time generation on a GPU. We also highlight that SoundCTM can achieve real-time generation on an Intel Xeon CPU with 2-step generation.

6.2 Training-Free Sound Intensity Control

To validate the proposed framework for training-free controllable T2S generation with SoundCTM, we conduct sound intensity control [Novack et al., 2024, Wu et al., 2023]. This task adjusts the dynamics of the generated sound to match a given target volume line or curve. We follow the experimental protocol from DITTO [Novack et al., 2024] to control the decibel (dB) volume line or curve of the generated samples.

We define $f(\mathbf{x}_0) := w * 20 \log 10(\text{RMS}(\mathbf{x}_0))$ in Eq. (6), where w represents the smoothing filter coefficients of a Savitzky-Golay filter [Savitzky and Golay, 1964] with a 1-second context window over the frame-wise value, and the RMS is the root mean squared energy of the generated sound. The target condition $\mathbf{y}_{\text{condition}}$ is a dB-scale target line or curve. We perform 70 iterations for \mathbf{z}_T -optimization following DITTO’s settings. Note that for the loss-based guidance framework, the \mathbf{z}_T -optimization is not conducted, which is much efficient. We set $\gamma = 0$ for sampling and evaluate the model performance with student EMA rate $\mu = 0.999$. We use 200 audio-text pairs from the AudioCaps testset for each of the 6 different types of $\mathbf{y}_{\text{condition}}$ as shown in Figure 4 (a) and Figure 6 (a). We evaluate our framework using the mean squared error (MSE) between the target and obtained $\mathbf{y}_{\text{condition}}$ to measure the accuracy of dynamics control, the FAD between generated samples and the entire AudioCaps testset, and the CLAP score. Experimental details are provided in Appendix B.2.

In Table 5, we compare results with various settings for SoundCTM’s controllable generation framework, as DITTO is not open-sourced. Firstly, overall, both \mathbf{z}_T -optimization and loss-based guidance frameworks effectively control intensity as indicated by the MSE results and the intensity curve shown in Figures 4 to 7. However, the FAD and CLAP scores are worse than those of the default T2S generation case. This is likely due to a degradation in auditory quality and a shift in the volume-conditioned audio distribution away from that of the AudioCaps testset. Additional results are provided in Appendix B.2.

⁷Since AudioLDM2-Large shows unreasonable RTF at a batch size of one, we also report the RTF at a batch size of eight, where the model does not suffer from this issue. Additionally, we use the "AudioLDM2-Full-Large" checkpoint instead of the AudioLDM2-AC-Large checkpoint, as the latter is not open-sourced. Note that the difference between "-AC-" and "-Full-" is in the training data.

Except for the MSE of 1-step with \mathbf{z}_T -optimization case, the loss-based guidance method outperforms \mathbf{z}_T -optimization method. Under 16-step cases, the loss-based guidance method shows better results than those of the optimization-based method across all the metrics. Interestingly, this finding contrasts with DITTO’s report that the optimization-based method outperforms the guidance-based one in terms of the MSE [Novack et al., 2024, Table 3]. The difference can be attributed to the performance improvement of the loss-based guidance method by using $G_{\theta}(\mathbf{z}_t, \mathbf{c}_{\text{txt}}, \omega, t, 0)$ instead of $\hat{\mathbf{z}}_0(\mathbf{z}_t)$, which provides a more accurate estimate of $\mathbf{z}_{0|t}$, resulting in more effective guidance during sampling. Considering both the qualitative results in Figures 4 to 7 and the quantitative results in Table 5, the loss-based guidance is the effective strategy for training-free controllable generation with SoundCTM.

7 Conclusion

We propose SoundCTM that achieves not only high-quality 1-step generation but also significantly improves sample quality by increasing the number of sampling steps with a single model. Our new training framework contributes to its performance. Our training-free controllable generation framework makes SoundCTM more controllable than just a fast T2S model. Furthermore, our frameworks, which does not rely on domain-specific components, has the potential to extend the applicability of CTM to a wider range of domains while maintaining both its fundamental methodology and impressive performance.

References

- Brian. D. O. Anderson. Reverse-time diffusion equation models. *Stochastic Processes and their Applications*, 12:313–326, 1982.
- Yatong Bai, Trung Dang, Dung Tran, Kazuhito Koishida, and Somayeh Sojoudi. Accelerating diffusion-based text-to-audio generation with consistency distillation. *arXiv preprint arXiv:2309.10740*, 2023.
- Keunwoo Choi, Jaekwon Im, Laurie Heller, Brian McFee, Keisuke Imoto, Yuki Okamoto, Mathieu Lagrange, and Shinosuke Takamichi. Foley sound synthesis at the dcase 2023 challenge. *In arXiv e-prints: 2304.12521*, 2023.
- Hyung Won Chung, Le Hou, Shayne Longpre, Barret Zoph, Yi Tay, William Fedus, Yunxuan Li, Xuezhi Wang, Mostafa Dehghani, Siddhartha Brahma, Albert Webson, Shixiang Shane Gu, Zhuyun Dai, Mirac Suzgun, Xinyun Chen, Aakanksha Chowdhery, Alex Castro-Ros, Marie Pellat, Kevin Robinson, Dasha Valter, Sharan Narang, Gaurav Mishra, Adams Yu, Vincent Zhao, Yanping Huang, Andrew Dai, Hongkun Yu, Slav Petrov, Ed H. Chi, Jeff Dean, Jacob Devlin, Adam Roberts, Denny Zhou, Quoc V. Le, and Jason Wei. Scaling instruction-finetuned language models, 2022.
- Bradley Efron. Tweedie’s formula and selection bias. *Journal of the American Statistical Association*, 106:1602 – 1614, 2011.
- Zach Evans, CJ Carr, Josiah Taylor, Scott H. Hawley, and Jordi Pons. Fast timing-conditioned latent audio diffusion. *arXiv preprint arXiv:2402.04825*, 2024.
- Deepanway Ghosal, Navonil Majumder, Ambuj Mehrish, and Soujanya Poria. Text-to-audio generation using instruction tuned llm and latent diffusion model. *arXiv preprint arXiv:2304.13731*, 2023.
- Sang gil Lee, Wei Ping, Boris Ginsburg, Bryan Catanzaro, and Sungroh Yoon. Bigvgan: A universal neural vocoder with large-scale training. In *Proc. International Conference on Learning Representation (ICLR)*, 2023.
- Ian J. Goodfellow, Jean Pouget-Abadie, Mehdi Mirza, Bing Xu, David Warde-Farley, Sherjil Ozair, Aaron Courville, and Yoshua Bengio. Generative adversarial networks. *Proc. Advances in Neural Information Processing Systems (NeurIPS)*, 2014.
- Great Big Story. The magic of making sound, 2017. URL https://www.youtube.com/watch?v=U03N_PRigX0.
- Kaiming He, Xiangyu Zhang, Shaoqing Ren, and Jian Sun. Deep residual learning for image recognition. In *Proc. IEEE Conference on Computer Vision and Pattern Recognition (CVPR)*, pages 770–778, 2016.
- Shawn Hershey, Sourish Chaudhuri, Daniel P. W. Ellis, Jort F. Gemmeke, Aren Jansen, R. Channing Moore, Manoj Plakal, Devin Platt, Rif A. Saurous, Bryan Seybold, Malcolm Slaney, Ron J. Weiss, and Kevin Wilson. Cnn architectures for large-scale audio classification. In *2017 IEEE International Conference on Acoustics, Speech and Signal Processing (ICASSP)*, pages 131–135, 2017.
- Jonathan Ho and Tim Salimans. Classifier-free diffusion guidance. *In arXiv e-prints: 2207.12598*, 2022.
- Jiawei Huang, Yi Ren, Rongjie Huang, Dongchao Yang, Zhenhui Ye, Chen Zhang, Jinglin Liu, Xiang Yin, Zejun Ma, and Zhou Zhao. Make-an-audio 2: Temporal-enhanced text-to-audio generation. *arXiv preprint arXiv:2305.18474*, 2023a.
- Rongjie Huang, Jiawei Huang, Dongchao Yang, Yi Ren, Luping Liu, Mingze Li, Zhenhui Ye, Jinglin Liu, Xiang Yin, and Zhou Zhao. Make-an-audio: Text-to-audio generation with prompt-enhanced diffusion models. *arXiv preprint arXiv:2301.12661*, 2023b.
- Vladimir Iashin and Esa Rahtu. Taming visually guided sound generation. In *British Machine Vision Conference (BMVC)*, 2021.

- Tero Karras, Miika Aittala, Timo Aila, and Samuli Laine. Elucidating the design space of diffusion-based generative models. In *Proc. Advances in Neural Information Processing Systems (NeurIPS)*, 2022.
- Kevin Kilgour, Mauricio Zuluaga, Dominik Roblek, and Matthew Sharifi. Fréchet audio distance: A metric for evaluating music enhancement algorithms. *arXiv preprint arXiv:1812.08466*, 2019.
- Chris Dongjoo Kim, Byeongchang Kim, Hyunmin Lee, and Gunhee Kim. AudioCaps: Generating Captions for Audios in The Wild. In *NAACL-HLT*, 2019.
- Dongjun Kim, Chieh-Hsin Lai, Wei-Hsiang Liao, Naoki Murata, Yuhta Takida, Toshimitsu Uesaka, Yutong He, Yuki Mitsufuji, and Stefano Ermon. Consistency trajectory models: Learning probability flow ode trajectory of diffusion. In *Proc. International Conference on Learning Representation (ICLR)*, 2024.
- Diederik P. Kingma and Jimmy Ba. Adam: A method for stochastic optimization. In *Proc. International Conference on Learning Representation (ICLR)*, 2017.
- Jungil Kong, Jaehyeon Kim, and Jaekyoung Bae. Hifi-gan: Generative adversarial networks for efficient and high fidelity speech synthesis. In *Proc. Advances in Neural Information Processing Systems (NeurIPS)*, 2020.
- Khaled Koutini, Jan Schlüter, Hamid Eghbal-zadeh, and Gerhard Widmer. Efficient training of audio transformers with patchout. In *Interspeech 2022, 23rd Annual Conference of the International Speech Communication Association, Incheon, Korea, 18-22 September 2022*, pages 2753–2757, 2022.
- Felix Kreuk, Gabriel Synnaeve, Adam Polyak, Uriel Singer, Alexandre Défossez, Jade Copet, Devi Parikh, Yaniv Taigman, and Yossi Adi. Audiogen: Textually guided audio generation. *Proc. International Conference on Learning Representation (ICLR)*, 2023.
- Rithesh Kumar, Prem Seetharaman, Alejandro Luebs, Ishaan Kumar, and Kundan Kumar. High-fidelity audio compression with improved rvqgan. In *Proc. Advances in Neural Information Processing Systems (NeurIPS)*, 2023.
- Mark Levy, Bruno Di Giorgi, Floris Weers, Angelos Katharopoulos, and Tom Nickson. Controllable music production with diffusion models and guidance gradients. *arXiv preprint arXiv:2311.00613*, 2023.
- Haohe Liu, Zehua Chen, Yi Yuan, Xinhao Mei, Xubo Liu, Danilo Mandic, Wenwu Wang, and Mark D Plumbley. AudioLDM: Text-to-audio generation with latent diffusion models. *Proc. International Conference on Machine Learning (ICML)*, 2023a.
- Haohe Liu, Qiao Tian, Yi Yuan, Xubo Liu, Xinhao Mei, Qiuqiang Kong, Yuping Wang, Wenwu Wang, Yuxuan Wang, and Mark D. Plumbley. AudioLDM 2: Learning holistic audio generation with self-supervised pretraining. *arXiv preprint arXiv:2308.05734*, 2023b.
- Liyuan Liu, Haoming Jiang, Pengcheng He, Weizhu Chen, Xiaodong Liu, Jianfeng Gao, and Jiawei Han. On the variance of the adaptive learning rate and beyond. In *Proc. International Conference on Learning Representation (ICLR)*, April 2020.
- Simian Luo, Chuanhao Yan, Chenxu Hu, and Hang Zhao. Diff-foley: Synchronized video-to-audio synthesis with latent diffusion models. In *Proc. Advances in Neural Information Processing Systems (NeurIPS)*, 2023.
- Navonil Majumder, Chia-Yu Hung, Deepanway Ghosal, Wei-Ning Hsu, Rada Mihalcea, and Soujanya Poria. Tango 2: Aligning diffusion-based text-to-audio generations through direct preference optimization. *arXiv preprint arXiv:2404.09956*, 2024.
- Zachary Novack, Julian McAuley, Taylor Berg-Kirkpatrick, and Nicholas J. Bryan. Ditto: Diffusion inference-time t-optimization for music generation. *arXiv preprint arXiv:2401.12179*, 2024.
- Robin Rombach, Andreas Blattmann, Dominik Lorenz, Patrick Esser, and Björn Ommer. High-resolution image synthesis with latent diffusion models. In *Proc. IEEE Conference on Computer Vision and Pattern Recognition (CVPR)*, 2022.

- Olaf Ronneberger, Philipp Fischer, and Thomas Brox. U-net: Convolutional networks for biomedical image segmentation. In Nassir Navab, Joachim Hornegger, William M. Wells, and Alejandro F. Frangi, editors, *Medical Image Computing and Computer-Assisted Intervention – MICCAI 2015*, pages 234–241, 2015.
- Tim Salimans, Ian Goodfellow, Wojciech Zaremba, Vicki Cheung, Alec Radford, and Xi Chen. Improved techniques for training gans. In *Proc. Advances in Neural Information Processing Systems (NeurIPS)*, 2016.
- Abraham. Savitzky and M. J. E. Golay. Smoothing and differentiation of data by simplified least squares procedures. *Analytical Chemistry*, 36(8):1627–1639, 1964.
- Takashi Shibuya, Yuhta Takida, and Yuki Mitsufuji. BigVSAN: Enhancing gan-based neural vocoders with slicing adversarial network. In *IEEE Int. Conf. Acoust., Speech, Signal Process. (ICASSP)*, 2024.
- Jascha Sohl-Dickstein, Eric A. Weiss, Niru Maheswaranathan, and Surya Ganguli. Deep unsupervised learning using nonequilibrium thermodynamics. In *Proc. International Conference on Machine Learning (ICML)*, 2015.
- J. Song, C. Meng, and S. Ermon. Denoising diffusion implicit models. *arXiv preprint arXiv:2010.02502*, 2020.
- Yang Song, Jascha Sohl-Dickstein, Diederik P Kingma, Abhishek Kumar, Stefano Ermon, and Ben Poole. Score-based generative modeling through stochastic differential equations. In *Proc. International Conference on Learning Representation (ICLR)*, 2021.
- Yang Song, Prafulla Dhariwal, Mark Chen, and Ilya Sutskever. Consistency models. *Proc. International Conference on Machine Learning (ICML)*, 2023.
- Zineng Tang, Ziyi Yang, Chenguang Zhu, Michael Zeng, and Mohit Bansal. Any-to-any generation via composable diffusion. In *Proc. Advances in Neural Information Processing Systems (NeurIPS)*, 2023.
- Pascal Vincent. A connection between score matching and denoising autoencoders. *Neural Computation*, 23(7):1661–1674, 2011.
- WIRED. How this woman creates god of war’s sound effects, 2023. URL <https://www.youtube.com/watch?v=WFVLWo5B81w>.
- Shih-Lun Wu, Chris Donahue, Shinji Watanabe, and Nicholas J. Bryan. Music controlnet: Multiple time-varying controls for music generation. *arXiv preprint arXiv:2311.07069*, 2023.
- Yusong Wu*, Ke Chen*, Tianyu Zhang*, Yuchen Hui*, Taylor Berg-Kirkpatrick, and Shlomo Dubnov. Large-scale contrastive language-audio pretraining with feature fusion and keyword-to-caption augmentation. In *IEEE International Conference on Acoustics, Speech and Signal Processing, ICASSP*, 2023.
- Jiwen Yu, Yinhuai Wang, Chen Zhao, Bernard Ghanem, and Jian Zhang. Freedom: Training-free energy-guided conditional diffusion model. *Proc. IEEE International Conference on Computer Vision (ICCV)*, 2023.
- Richard Zhang, Phillip Isola, Alexei A. Efros, Eli Shechtman, and Oliver Wang. The unreasonable effectiveness of deep features as a perceptual metric. In *Proc. IEEE Conference on Computer Vision and Pattern Recognition (CVPR)*, 2018.
- Alon Ziv, Itai Gat, Gael Le Lan, Tal Remez, Felix Kreuk, Alexandre Défossez, Jade Copet, Gabriel Synnaeve, and Yossi Adi. Masked audio generation using a single non-autoregressive transformer. *arXiv preprint arXiv:2401.04577*, 2024.

A Related Work

Masked Audio Token Modeling AudioGen [Kreuk et al., 2023] and MAGNeT [Ziv et al., 2024] utilize masked generative sequence modeling of discrete audio tokens for T2S generation. These models exhibit a trade-off between sample quality and inference speed due to their token prediction methods. AudioGen provides better sample quality but requires much more time for sample generation due to its autoregressive prediction. In contrast, MAGNeT offers faster inference through its non-autoregressive prediction.

Diffusion-based Models Recent literature [Huang et al., 2023b,a, Liu et al., 2023a,b, Ghosal et al., 2023, Evans et al., 2024] and competitions [Choi et al., 2023] report that LDM-based sound generation models outperform other approaches such as GANs. For fast generation, ConsistencyTTA [Bai et al., 2023] and Stable Audio [Evans et al., 2024] employ efficient strategies. Stable Audio, for instance, compresses a 95-second waveform signal to a latent representation, allowing its LDM to generate the representation through a multi-step reverse-time process, unlike other models that compress only 10-second audio signals.

Training-free Controllable Generation Levy et al. [2023] demonstrate training-free controllable music generation using loss-based guidance [Yu et al., 2023]. Their approach defines a task-specific loss, such as for music continuation and infilling, and incorporates the gradient of this loss into the reverse-time diffusion process. Novack et al. [2024] also present controllable generation by optimizing initial noisy latents based on loss computed in the target condition space. During optimization, diffusion models perform a reverse-time process to obtain a clean signal, which is projected onto the condition space by a predefined differentiable feature extractor. Post-optimization, the model generates a music signal from the optimized initial latent.

B Experimental Details

B.1 Details of T2S Generation

Training Details For teacher’s training, we use $\sigma_{\text{data}} = 0.25$ and time sampling $t \sim \mathcal{N}(-1.2, 1.2^2)$ by following EDM’s training manner. We mostly follow the original CTM’s training setup for student training. We utilize the EDM’s skip connection $c_{\text{skip}}(t) = \frac{\sigma_{\text{data}}^2}{t^2 + \sigma_{\text{data}}^2}$ and output scale $c_{\text{out}}(t) = \frac{t\sigma_{\text{data}}}{\sqrt{t^2 + \sigma_{\text{data}}^2}}$ for g_{θ} modeling as

$$g_{\theta}(\mathbf{z}_t, \mathbf{c}_{\text{text}}, \omega, t, s) = c_{\text{skip}}(t)\mathbf{z}_t + c_{\text{out}}(t)\text{NN}_{\theta}(\mathbf{z}_t, \mathbf{c}_{\text{text}}, \omega, t, s),$$

where NN_{θ} refers to the actual neural network output. We initialize the student’s NN_{θ} with ϕ except for student model’s s -embedding and ω -embedding structure.

We use 8×NVIDIA H100 (80G) GPUs and a global batch size of 64 for the training. We choose t and s from the N -discretized timesteps to calculate $\mathcal{L}_{\text{CTM}}^{\text{Sound}}$. For $\mathcal{L}_{\text{DSM}}^{\text{Sound}}$ calculation, we opt to use 50% of time sampling $t \sim \mathcal{N}(-1.2, 1.2^2)$. For the other half time, we first draw sample from $\xi \sim [0, 0.7]$ and transform it using $(\sigma_{\text{max}}^{1/\rho} + \xi(\sigma_{\text{min}}^{1/\rho} - \sigma_{\text{max}}^{1/\rho}))^{\rho}$. We apply Exponential Moving Average (EMA) to update $\text{sg}(\theta)$ by

$$\text{sg}(\theta) \leftarrow \text{stopgrad}(\mu \text{sg}(\theta) + (1 - \mu)\theta).$$

Throughout the experiments, for student training, we use $N = 40$, $\mu = 0.999$, $\sigma_{\text{min}} = 0.002$, $\sigma_{\text{max}} = 80$, $\rho = 7$, RAdam optimizer [Liu et al., 2020] with a learning rate of 8.0×10^{-5} , and $\sigma_{\text{data}} = 0.25$. We set the maximum number of ODE steps as 39 during training and we use Heun solver for $\text{Solver}(\mathbf{z}_t, \mathbf{c}_{\text{text}}, \omega, t, u; \phi)$. To obtain the results shown in Table 6 and Figure 1, SoundCTM was trained for 30 K iterations. For other results, models were trained for 18 K iterations. We also utilized TANGO’s data augmentation [Ghosal et al., 2023, Sec. 2.3] during student training.

The network architecture and dataset for the teacher’s training remained unchanged from the original ones. Our teacher model (TANGO) and SoundCTM share the overall model architecture, comprising the VAE-GAN [Liu et al., 2023a], the HiFiGAN vocoder [Kong et al., 2020] as \mathcal{D} and the Stable Diffusion UNet architecture (SD-1.5), which consists of 9 2D-convolutional ResNet [He et al., 2016] blocks as D_{ϕ} . The UNet has a total of 866 M parameters, and the frozen FLAN-T5-Large text encoder [Chung et al., 2022] is used. The UNet employs 8 latent channels and a cross-attention dimension of 1024. For \mathcal{D} in SoundCTM, we used the AudioLDM1 checkpoint by following TANGO.

Table 7: Quantitative results of sound intensity control on SoundCTM

# of steps	\mathbf{z}_T optimization	Loss guidance	γ	MSE↓	FAD _{vgg} ↓	CLAP ↑
Default 16-step T2S Generation	X	X	0	231.9	2.08	0.47
1	✓	X	0	6.57	4.94	0.34
16	✓	X	0	60.2	3.65	0.38
16	✓	X	0.2	50.4	3.71	<u>0.41</u>
16	X	✓	0	18.5	3.04	<u>0.41</u>
16	X	✓	0.2	14.2	<u>3.58</u>	0.42
16	✓	✓	0	<u>10.7</u>	4.34	0.37

Evaluation Details For large-NFE sampling, we follow the EDM’s and the CTM’s time discretization. Namely, if we draw n -NFE samples, we equi-divide $[0, 1]$ with n points and transform it (say ξ) to the time scale by $(\sigma_{\max}^{1/\rho} + (\sigma_{\min}^{1/\rho} - \sigma_{\max}^{1/\rho})\xi)^\rho$. However, we emphasize the time discretization for both training and sampling is a modeler’s choice.

Algorithm 2 SoundCTM’s Training

Require: Probability of unconditional training p_{uncond}

```

1: repeat
2:   Sample  $(\mathbf{x}_0, \mathbf{c}_{\text{text}})$  from  $p_{\text{data}}$ 
3:   Calculate  $\mathbf{z}_0$  through  $\mathcal{E}(\mathbf{x}_0)$ 
4:    $\mathbf{c}_{\text{text}} \leftarrow \emptyset$  with  $p_{\text{uncond}}$ 
5:   Sample  $\epsilon \sim \mathcal{N}(0, I)$ 
6:   Sample  $t \in [0, T]$ ,  $s \in [0, t]$ ,  $u \in [s, t]$ 
7:   Sample  $\omega \sim U[\omega_{\min}, \omega_{\max}]$ 
8:   Calculate  $\mathbf{z}_t = \mathbf{z}_0 + t\epsilon$ 
9:   Calculate  $\text{Solver}(\mathbf{z}_t, \mathbf{c}_{\text{text}}, \omega, t, u; \phi)$ 
10:  Calculate  $\mathbf{z}_{\text{target}}(\mathbf{z}_t, \mathbf{c}_{\text{text}}, \omega, t, u, s)$ 
11:  Calculate  $\mathbf{z}_{\text{est}}(\mathbf{z}_t, \mathbf{c}_{\text{text}}, \omega, t, s)$ 
12:  Update  $\theta \leftarrow \theta - \frac{\partial}{\partial \theta} \mathcal{L}(\theta)$ 
13: until converged

```

Algorithm 3 SoundCTM’s Inference

Require: $\nu, \mathbf{c}_{\text{text}}, \omega$,
Hyperparameter of CTM’s γ -sampling γ

```

1: Sample  $\mathbf{z}_{t_0}$  from prior distribution
2: for  $n = 0$  to  $N - 1$  do
3:    $\tilde{t}_{n+1} \leftarrow \sqrt{1 - \gamma^2} t_{n+1}$ 
4:    $\mathbf{z}_{\tilde{t}_{n+1}} \leftarrow \nu G_\theta(\mathbf{z}_{t_n}, \mathbf{c}_{\text{text}}, \omega, t_n, \tilde{t}_{n+1})$ 
5:    $+ (1 - \nu) G_\theta(\mathbf{z}_{t_n}, \emptyset, \omega, t_n, \tilde{t}_{n+1})$ 
6:    $\mathbf{z}_{t_{n+1}} \leftarrow \mathbf{z}_{\tilde{t}_{n+1}} + \gamma t_{n+1} \epsilon$ 
7: end for
8: Return  $\mathbf{z}_{t_N}$ 

```

B.2 Details of Sound Intensity Control

During the SoundCTM’s optimization-based framework, we use Adam [Kingma and Ba, 2017] with a learning rate of 1.0. We also tested learning rates of 1.0×10^{-1} , 1.0×10^{-2} , and 5.0×10^{-3} by following DITTO. However, we cannot obtain better results than the case using 1.0. For the time-dependent learning rate ρ_t in SoundCTM’s loss-based guidance framework, we use the overall gradient norm by following DITTO.

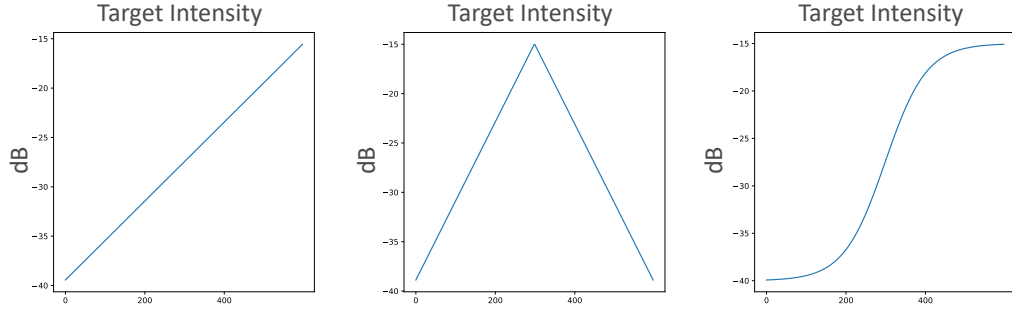
We set $\nu = 1$ for 1-step generation with \mathbf{z}_T -optimization, $\nu = 2$ for both 16-step generation with \mathbf{z}_T -optimization and 16-step loss-based guidance, and $\omega = 3.5$ for all the settings. The same values of $\nu = 2$ and $\omega = 3.5$ are used for the default 16-step T2S generation. For time discretization in multi-step generation, we use the same scheme as in T2S generation evaluation.

In Table 7, we present additional results of sound intensity control. In addition to Table 5, we include results using stochastic sampling ($\gamma = 0.2$). Furthermore, we report results incorporating loss-based guidance after \mathbf{z}_T -optimization. Overall, stochastic sampling did not yield significant performance improvement. Integrating the loss-based guidance framework with \mathbf{z}_T -optimization showed the better MSE, consistent with DITTO’s findings, but resulted in the much worse FAD and CLAP scores compared with only using the loss-based guidance.

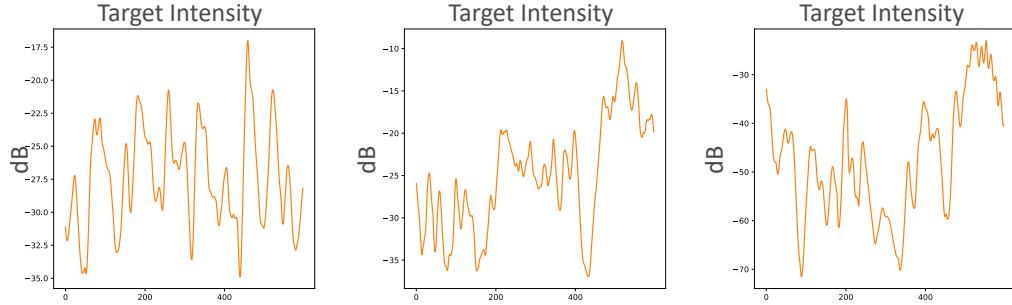
Algorithm 4 SoundCTM’s optimization-based training-free controllable generation framework

Require: $\nu, \mathbf{c}_{\text{text}}, \omega, \mathbf{y}_{\text{condition}}, \gamma$, Learning rate ρ_{t_n}

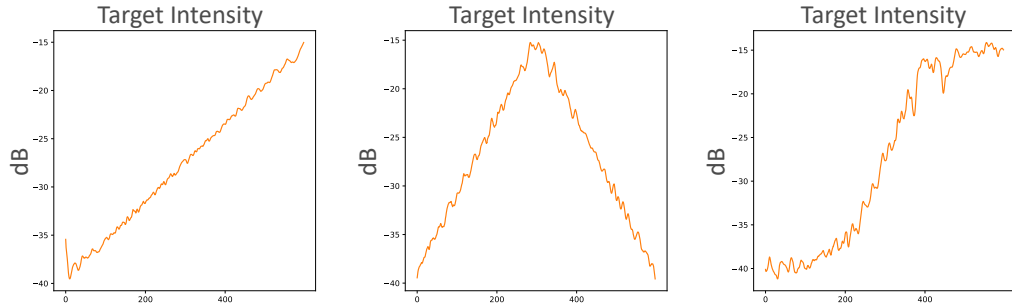
```
1: Sample  $\mathbf{z}_{t_0} \sim \mathcal{N}(0, I)$ 
2: // Run optimization
3: for  $k = 0$  to  $K - 1$  do
4:   Denoise  $\mathbf{z}_{t_N} \leftarrow G_{\theta}(\mathbf{z}_{t_0}, \mathbf{c}_{\text{text}}, \omega, t_0, 0)$ 
5:    $\hat{\mathbf{y}}_{\text{condition}} = f(\mathcal{D}(\mathbf{z}_{t_N}))$ 
6:   Update  $\mathbf{z}_{t_0} \leftarrow \mathbf{z}_{t_0} - \rho_{t_n} \nabla_{\mathbf{z}_{t_0}} \mathcal{L}(\hat{\mathbf{y}}_{\text{condition}}, \mathbf{y}_{\text{condition}})$ 
7: end for
8: // Run generation from optimized  $\mathbf{z}_{t_0}^*$ 
9: Start from  $\mathbf{z}_{t_0}^*$ 
10: for  $n = 0$  to  $N - 1$  do
11:    $\tilde{t}_{n+1} \leftarrow \sqrt{1 - \gamma^2} t_{n+1}$ 
12:    $\mathbf{z}_{\tilde{t}_{n+1}} \leftarrow \nu G_{\theta}(\mathbf{z}_{t_n}, \mathbf{c}_{\text{text}}, \omega, t_n, \tilde{t}_{n+1})$ 
13:    $+ (1 - \nu) G_{\theta}(\mathbf{z}_{t_n}, \emptyset, \omega, t_n, \tilde{t}_{n+1})$ 
14:    $\mathbf{z}_{t_{n+1}} \leftarrow \mathbf{z}_{\tilde{t}_{n+1}} + \gamma t_{n+1} \epsilon$ 
15: end for
16: Return  $\mathbf{z}_{t_N}$ 
```



(a) Target intensities



(b) Default T2S generation



(c) z_T -optimization with 1-step generation



(d) z_T -optimization with 16-step generation

Figure 4: Target sound intensities (blue) and obtained intensities (orange). We use the same text prompt within each column and different prompts across different columns. Note that we use 70 iterations for z_T -optimization.

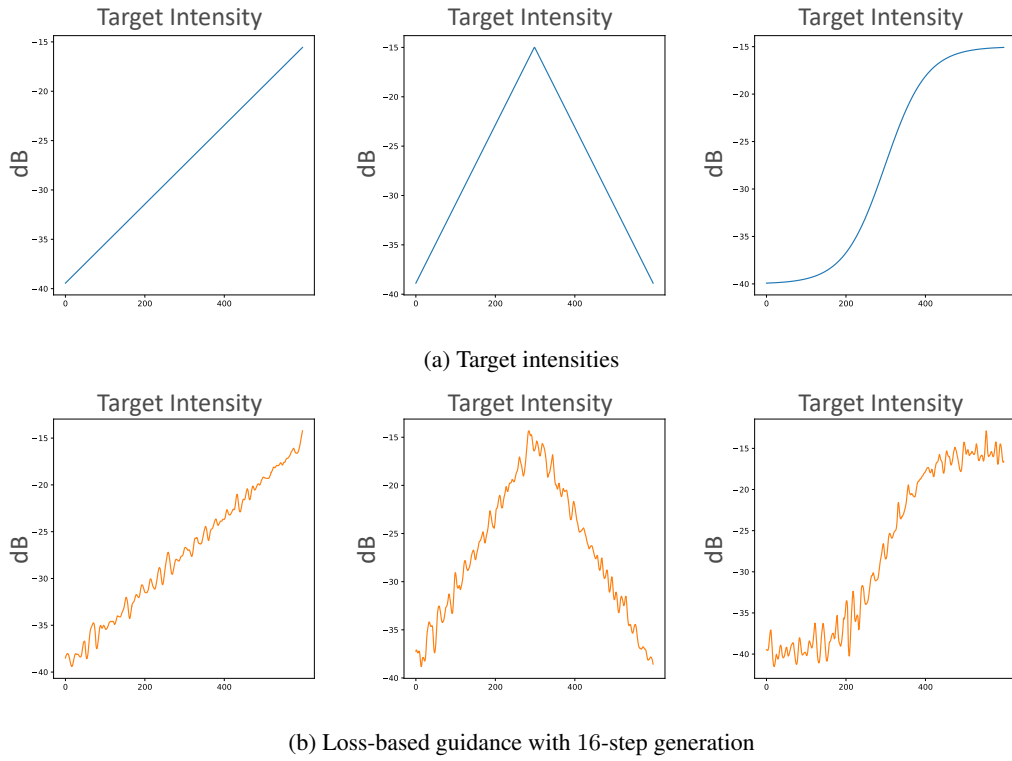
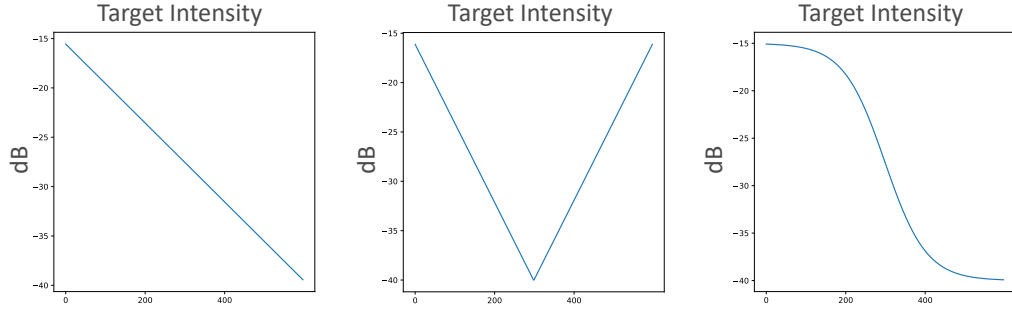
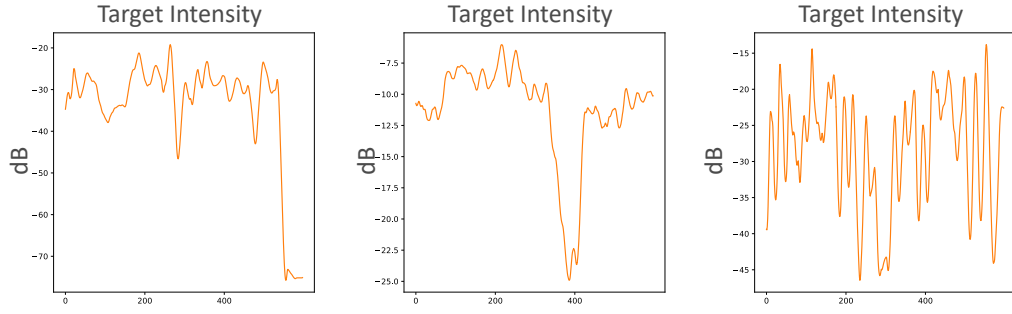


Figure 5: Target sound intensities (blue) and obtained intensities (orange). We use same text prompts within each column and different prompt for each different column.



(a) Target intensities



(b) Default T2S sound generation



(c) z_T -optimization with 1-step generation



(d) z_T -optimization with 16-step generation

Figure 6: Target sound intensities (blue) and obtained intensities (orange). We use the same text prompt within each column and different prompts across different columns. Note that we use 70 iterations for z_T -optimization.

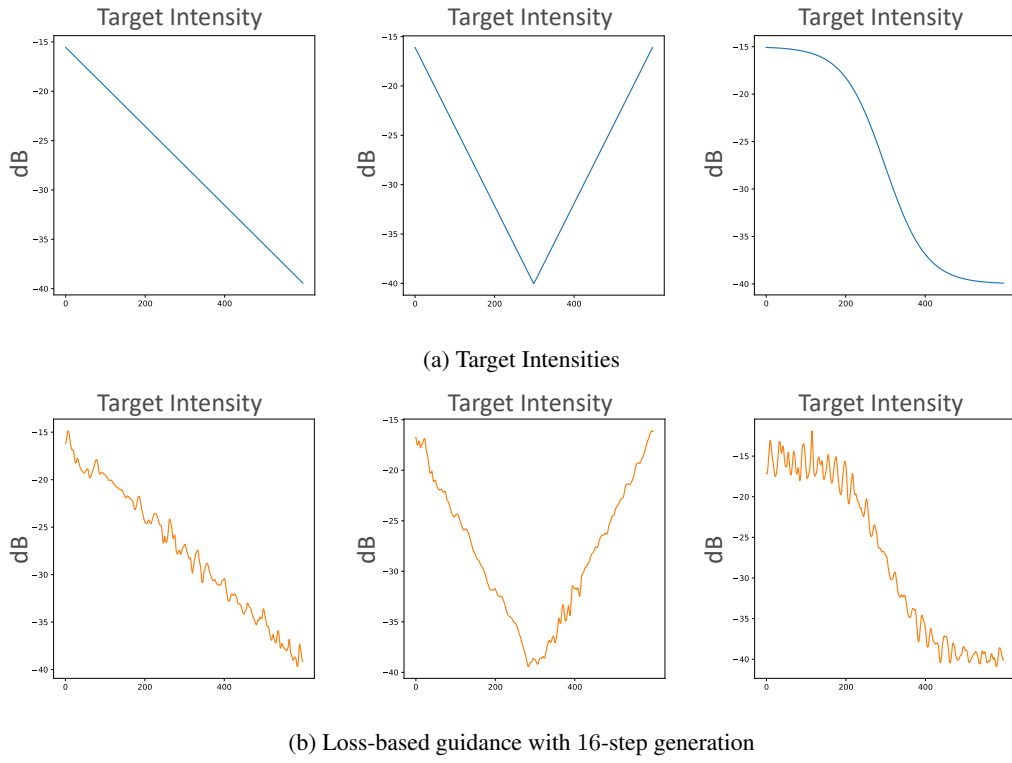


Figure 7: Target sound intensities (blue) and obtained intensities (orange). We use the same text prompt within each column and different prompts across different columns.